Discontinuous Wing Leading Edge to Enhance Spin Resistance

Daniel J. DiCarlo,* Kenneth E. Glover,* Eric C. Stewart,† and H. Paul Stough†
NASA Langley Research Center, Hampton, Virginia

Spin resistance of two typical general-aviation airplanes has been studied. Improvement in spin resistance due to an outboard wing leading-edge modification was evaluated through wind tunnel and flight tests. The basic airplanes would readily enter a spin; however, with the wing modification the airplanes were highly spin resistant. Spin resistance has been related to the angle of attack of the outer wing panel and the yaw rate as a step toward development of guidelines for design of more spin-resistant airplanes.

Nomenclature

b = wing span, ft
$\bar{c}$ = mean aerodynamic chord, ft
C_D = drag coefficient, drag/qS
$C_{D_{ow}}$ = outer wing drag coefficient, outer wing drag/qS_{ow}
C_L = lift coefficient, lift/qS
$C_{L_{ow}}$ = outer wing lift coefficient, outer wing lift/qS_{ow}
C_R = total resultant-force coefficient, $\sqrt{C_L^2 + C_D^2}$
$C_{R_{ow}}$ = outer wing panel resultant-force coefficient, $\sqrt{C_{l_{ow}}^2 + C_{D_{ow}}^2}$
q = dynamic pressure, psf
S = wing area, ft^2
S_{ow} = outer wing area, ft^2
α = angle of attack, deg

Introduction

NASA Langley Research Center is conducting research to develop the technology required to improve the stall/spin characteristics of light general-aviation airplanes. Much of this effort has focused on wing aerodynamics and has resulted in a wing leading-edge modification that significantly improved the stall/spin behavior of three research airplanes. This modification consists of a discontinuous drooped leading edge added to the outboard wing section, which increased the stall angle of the outer wing panel and enhanced spin resistance. The leading-edge design was initially developed on an untwisted rectangular wing[1-3] and, as presented herein, subsequently was applied to a twisted rectangular wing and a twisted tapered wing.

Flight tests of airplanes that would readily enter a spin in their basic configuration indicated that with the addition of the wing modification the airplanes had an increased resistance to enter a spin, particularly within the normal loading envelope. Providing such increased spin resistance may improve the safety of this class of airplane by significantly reducing the chance of inadvertently entering a spin.

The typical stall departure and spin entry is marked by a roll-off which significantly increases angle of attack on the downgoing wing, further aggravating the stalled condition and promoting autorotation. Therefore, the initial investigation of spin resistance using this wing modification[4] concentrated on an analysis of local angle of attack of the outer wing panel of the downgoing wing. It was assumed that if the local angle of attack never exceeded the stall value for the outer panel, the airplane could not spin. The analysis tended to confirm this assumption for that particular airplane, but it was noted that the angle of attack could exceed the stall value momentarily without resulting in a spin.

Because of the apparent limitations of this simplified approach, the present paper extends the spin-resistance analysis to a second airplane and adds consideration of other lateral-directional motions. In particular, the apparent importance of yawing motions at high angles of attack is discussed relative to departure and spin resistance.

Test Configurations

Two single-engine, low-wing, general-aviation airplanes were used for this investigation. One had a twisted, tapered wing and T-tail configuration, as shown in Fig. 1, referred to herein as airplane T (tapered wing). The second airplane had a twisted rectangular wing and low horizontal tail, as shown in Fig. 2, referred to as airplane R (rectangular wing). The physical characteristics of each airplane are given in Table 1. Each airplane was equipped with a tail-mounted spin-recovery parachute system. Ballast was used to vary weight, center-of-gravity position, and moments of inertia.

The wing leading-edge modification used on both airplanes was similar to that used in the earlier tests of Ref. 1. On airplane T, the modification consisted of drooping the leading edge from the 53 to 96% semispan location, as shown in Fig. 3. The basic wing had an NACA 65_2415 airfoil and incorporated some leading-edge droop, which increased from no droop at the start of the taper to a maximum at the wing tip. The 2 deg of washout across the tapered panel of the basic wing was increased to 8.5 deg for the modified outboard leading-edge configuration. When added to airplane R, whose basic wing has a 63_2A415 airfoil, the leading-edge modification extended from the 54 to 97% semispan locations, as shown in Fig. 4, and maintained the 2 deg of washout over the outer panels of the basic wing.

Wind Tunnel Tests

Tests were conducted in the Langley 12-ft Low-Speed Wind Tunnel to identify wing leading-edge designs that would improve high angle-of-attack characteristics.[1,5] The wing leading-edge modification was developed with the added objectives of low cost, light weight, no maintenance, and minimal impact on performance. Aerodynamic data were measured over an angle-of-attack range of -4 to $+60$ deg at a Reynolds number of 320,000 based on wing chord. Forces and moments were measured separately for the total model and for the outer 50% of the wing.

Received May 11, 1984; revision received Dec. 19, 1984. This paper is declared a work of the U.S. Government and therefore is in the public domain.

*Research Engineer, Low-Speed Aerodynamics Division.
†Research Engineer, Low-Speed Aerodynamics Division. Member AIAA.

An outboard wing leading-edge droop modification with the droop beginning just outboard of the midsemispan had the most favorable effect on high angle-of-attack characteristics within the constraints imposed. Figures 5 and 6 show the total and outer wing panel resultant-force coefficient (combination of lift and drag) as a function of angle of attack for 1/6-scale models of the test configurations. Results indicate similar trends for both models. For the basic wings, outer panel stall occurs at about 15 to 18-deg angle of attack as noted by the sharp reduction in resultant force, reflecting the decrease of lift as angle of attack is increased beyond the stall. This change to a negative resultant-force curve slope at the higher angles of attack is indicative of unstable roll damping and a tendency for the airplane to spin.[6]

Addition of the wing modification has a negligible effect on the resultant-force coefficient at low angles of attack. Beyond the stall angle of attack of the basic wing, however, the lift of the modified outer wing panel continues to increase and produces a positive (stabilizing) resultant-force slope up to 30 to 35-deg angle of attack. As with the basic wing, separation of flow on the inboard portion of the wing would produce buffet for stall warning; however, unlike the basic wing the lift on the modified outer panel continues to increase, enabling penetration beyond the perceived stall. These characteristics are due to the outer panel acting like an isolated, low-aspect ratio wing at the higher angles of attack.[3]

Flow-Visualization Tests

Oil-flow studies at the University of Maryland using a 1/6-scale model of airplane T provided further understanding of the flow characteristics produced by the discontinuous leading-edge droop which result in the increase in stall angle of attack of the outer wing panel. As seen in Fig. 7a, stall of the basic tapered wing starts at the root trailing edge and progresses forward and outboard as the angle of attack is increased. At 30-deg angle of attack (Fig. 7b), the flow is separated and the spanwise flow of the boundary layer is evidenced by the surface patterns.

Table 1 Physical characteristics of test aircraft

	Airplane T	Airplane R
Engine		
Type	4 cylinder horizontally opposed	4 cylinder horizontally opposed
Rated continuous power, hp	200	180
Rated continuous speed, rpm	2700	2700
Propeller		
Type	2 blades, constant speed	2 blades fixed pitch
Diameter, in.	76	76
Pitch, (variable)	14-31 deg	60 in.
Overall dimensions		
Span, ft	35.43	32.75
Length, ft	27.80	25.73
Height, ft	8.26	8.20
Wing (basic)		
Area, ft^2 total	173.70	145.63
Outer panel area, ft^2	38.50	33.08
Root chord, ft	6.17	4.39
Tip chord, ft	3.52	4.39
Mean aerodynamic chord, ft	5.18	4.39
Aspect ratio	7.24	7.36
Dihedral, deg	7.0	6.5
Incidence		
Root, deg	2.0	3.0
Tip, deg	−1.0	1.0
Airfoil section	NACA $65_2$415 modified	NACA 63_2A415
Stabilator		
Span, ft	10.0	10.8
Root chord, ft	2.5	2.5
Tip chord, ft	2.5	2.5
Airfoil section	NACA 0012	NACA 63A012 modified
Vertical tail		
Span, ft	5.07	4.61
Tail offset, deg	0.0	0.0
Root chord, ft	4.54	4.52
Tip chord, ft	2.38	1.81
Control surface deflections		
Stabilator, deg	10 up, 10 down	15 up, 2 down
Aileron, deg	30 up, 16 down	20 up, 10 down
Rudder, deg	30 left, 30 right	25 left, 25 right
Flap, deg	0,40 down	0, 35 down
Gross weight, lb	2750	2450
Test weight at altitude, lb	2690	2390
Center-of-gravity position, % $\bar{c}$	28	23
Moments of inertia about body axes		
Ix, slug-ft^2	2246	1700
Iy, slug-ft^2	2495	1920
Iz, slug-ft^2	4253	3200

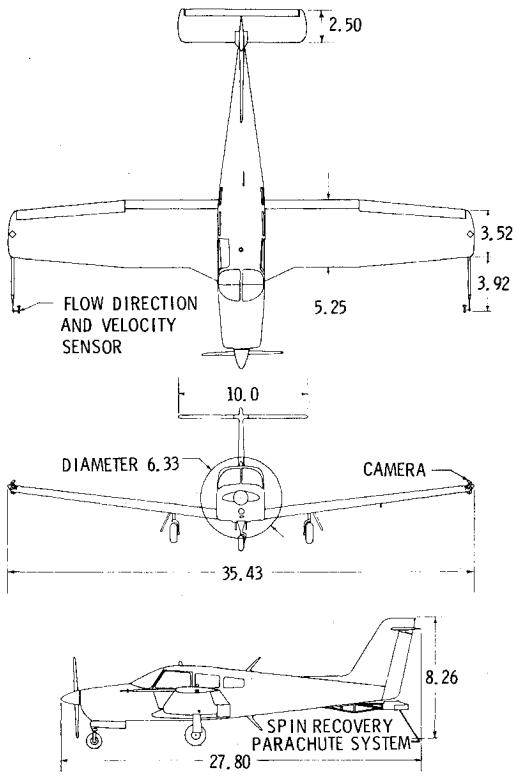

Fig. 1 Test airplane T (dimensions in feet).

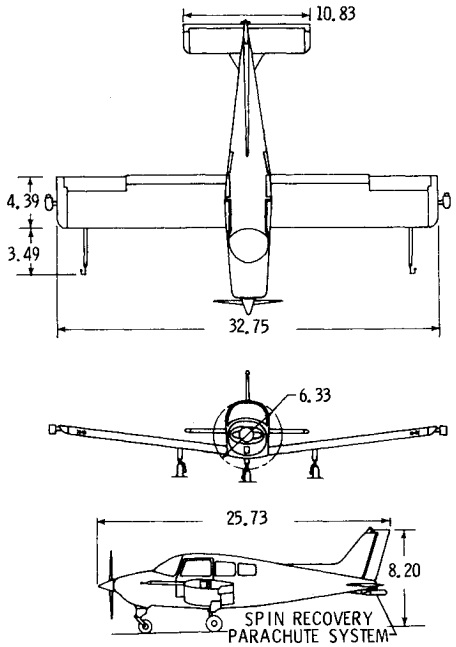

Fig. 2 Test airplane R (dimensions in feet).

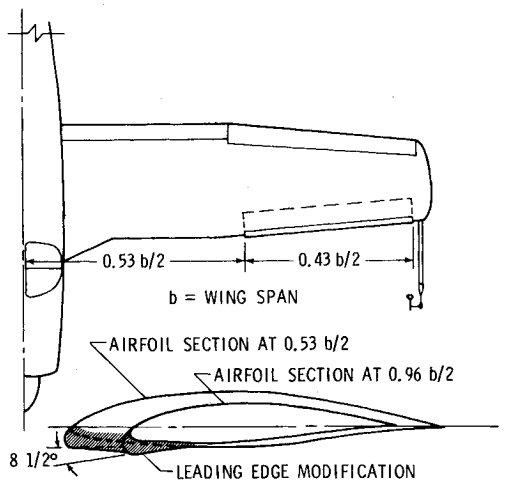

Fig. 3 Wing leading-edge modification to outboard wing panel of airplane T.

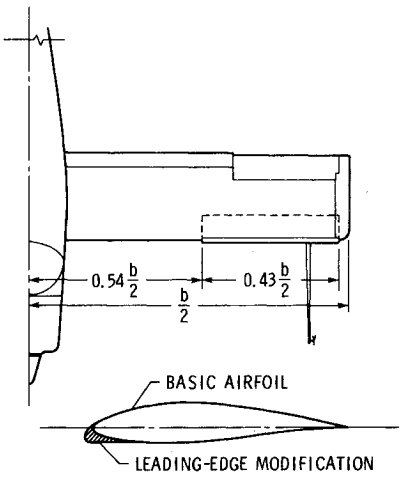

Fig. 4 Wing leading-edge modification to outboard wing panel of airplane R.

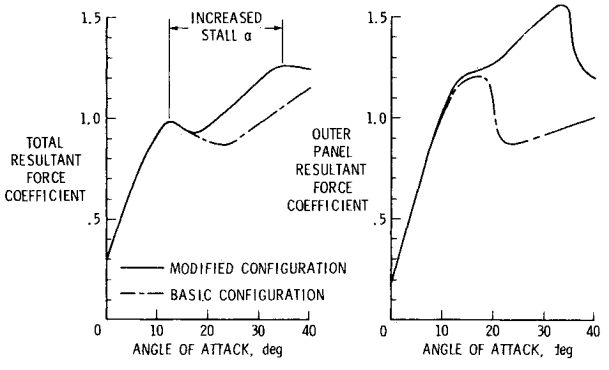

Fig. 5 Resultant force coefficients for airplane T (1/6-scale model).

With the outboard wing modification, the flow on the inboard panel, Fig. 7c, is similar to that of the basic wing at about 16-deg angle of attack, but the separation does not progress spanwise to the modified outer panel as angle of attack is increased to 35 deg, Fig. 7d. Closer examination of the photographs shows a vortex-type flow emanating from the leading-edge discontinuity which seems to prevent outward progression of the separated flow. Maintaining attached flow on the outer panel would thus result in an increased stall angle of attack and improved departure characteristics. Generally, these oil-flow results show trends similar to those noted during earlier oil-flow studies of an untwisted rectangular wing and are consistent with the aerodynamic data presented.

Flight-Test Results

Flight tests were performed at the NASA Wallops Flight Center. Spin entries were attempted at altitudes between 9000 and 12,000 ft with recoveries completed above 5000 ft. For each airplane over 125 spin entries were attempted for each

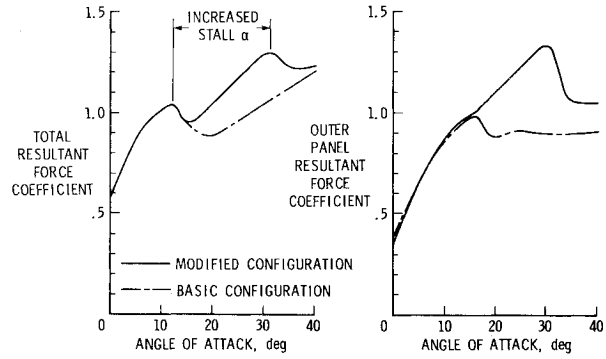

Fig. 6 Resultant force coefficients for airplane R (1/6-scale model).

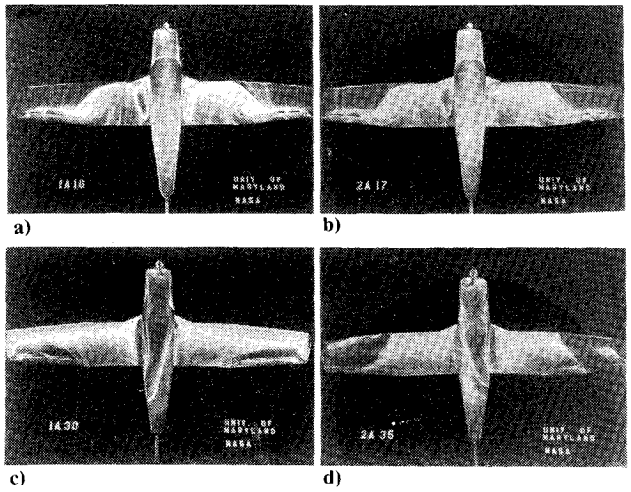

Fig. 7 Oil-flow visualization (1/6-scale model of airplane T): a) Basic wing, 16-deg angle of attack, b) Basic wing, 30-deg angle of attack, c) Modified wing, 17-deg angle of attack, d) Modified wing, 35-deg angle of attack.

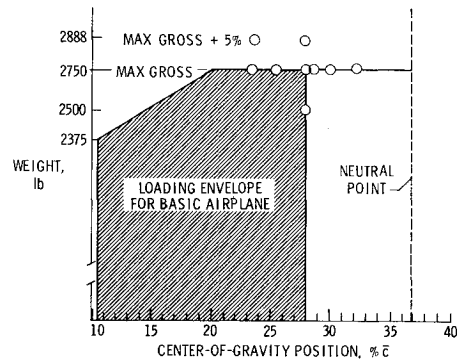

Fig. 8 Loading conditions for flight tests of airplane T with wing modification.

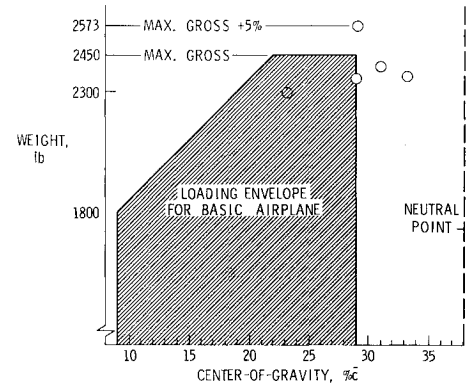

Fig. 9 Loading conditions for flight tests of airplane R with wing modification.

test configuration, for a variety of entry conditions. Flight Reynolds numbers at the stall ranged from 3.0 to 3.8×10^6 based on wing chord.

The airplanes were instrumented to measure and record true airspeed and flow angles ahead of each wing tip, linear accelerations and angular rates along and about the body axes, control positions and forces, engine power parameters, altitude, and dynamic pressure. The onboard data system was supplemented by ground video and movie camera coverage and wing-tip and cockpit-mounted cameras. Pilot comments, via radio, were recorded on the ground video tape. All data were time correlated and provided a continuous time history from maneuver entry through recovery.

The neutral point of airplane T was at 36.6% mean aerodynamic chord (mac), both power-on and power-off. Initial spin tests were conducted at a nominal aft center-of-gravity position of 28% mac (8.6% static margin) and weight of 2500 lb. The circles on Fig. 8 denote the weight and center-of-gravity positions for additional tests of the modified airplane, most of which were conducted at 2750 lb (maximum gross weight). The neutral point for airplane R was at 38.0% mac, both power-on and power-off. Weight and center-of-gravity combinations for tests of airplane R are shown in Fig. 9.

Stall characteristics of the basic airplanes were somewhat docile and well behaved. A poststall wing rock was noted, prior to reaching full-aft stick position, which tended to develop into an uncontrollable rolloff. Both airplanes would readily spin from 1-*g* flight, power-on or power-off with the application of normal prospin controls (full-aft stick followed by prospin rudder, ailerons neutral). Airplane T spun at about 43-deg angle of attack; airplane R had two spin modes and spun either at about 39- or 55-deg angle of attack. Application of recovery controls would not always stop the spins.

With the wing modification, stall characteristics improved such that the pilot was able to penetrate the stall to full-aft stick and control any rolloff with normal use of aileron or rudder. Both airplanes achieved a steady, wings-level descent at an angle of attack greater than the basic airplane stall. When spins were attempted, both airplanes were very difficult to spin unless prolonged, aggravated control inputs or abused loadings were employed. Modified airplane T did not spin at idle power for any loading or maneuver tested. At midrange center-of-gravity loadings with maximum power, a zoom entry with properly timed prospin control inputs was needed to enter a spin. Only when modified airplane T was loaded beyond the approved loading envelope in combination with maximum power could a spin be entered from a 1-*g* stall.

Regardless of power or type of maneuver, modified airplane R did not spin within the normal loading envelope. Movement of the center of gravity to aft of the approved limits enabled spin entry from a zoom maneuver. Additional aft movement of the center of gravity was required before modified airplane R entered a spin from a 1-*g* stall. For both airplanes, when spins were obtained, they tended to be flatter and recover slower than those of the basic airplanes.

Spin resistance was improved significantly for both airplanes, as evidenced by comparing the frequency with which each would enter a spin following prospin control inputs for both the basic and modified configurations. Specifically, for basic airplane T, 224 of 255 (88%) attempted spins resulted in spins; for basic airplane R, 127 of 129 (98%) attempted spins resulted in spins. With the wing modification for airplane T, only 12 of 236 (5%) attempted spins resulted in

spins, and for airplane R only 7 of 134 (5%) attempted spins resulted in spins. These percentages for the modified airplanes would be more impressive if only spin attempts from a 1-g stall were considered. As noted previously, a majority of the spins obtained with the wing modification, especially within the normal operating envelopes of both airplanes, did consistently require certain aggravated control inputs.

Analysis of Spin Resistance

As noted in Ref. 4, initial analysis of spin resistance of an airplane with the outboard wing modification involved the assumptions that 1) an airplane would be highly spin resistant if roll damping could be maintained for all maneuvers, and 2) roll damping could be maintained if the outer wing panel did not stall. Conceptually, spin resistance was thus related to the difference between the maximum attainable angle of attack and stall angle of attack. The maximum attainable angle of attack was defined as the maximum angle of attack of the downgoing wing outer panel, including dynamic effects, while the stall angle of attack was defined as the local angle of attack at which the outer panel flow separated. For analysis purposes, maximum attainable angle of attack was divided into a baseline trim angle of attack and increments due to center-of-gravity changes, power effects, and dynamic effects. If the summation of these increments did not exceed the outer panel stall angle of attack, then the airplane would not be expected to spin. However, it was found that during many maneuvers the stall angle of attack could be exceeded temporarily without leading to a spin entry. Thus, requiring the angle of attack to never exceed the stall value for all conceivable maneuvers would be overly restrictive.

As a first step in refining the analysis process, the techniques of Ref. 4 were applied to the test results of the two airplanes. The outer wing stall angle of attack was determined from measured angle-of-attack data and corresponding films of tufts on the wings. These values for the basic and modified airplane configurations are indicated by the horizontal lines in Figs. 10 and 11. The static trim angles of attack with full nose-up pitch control input were measured for a range of center-of-gravity positions at maximum gross weight with maximum power and idle power for the modified airplanes. Results are presented in Figs. 10 and 11 as plots of static trim angle of attack vs center-of-gravity position. Regions above the static trim curves, denoted by the arrows, represent the transient effects of the dynamics associated with the spin entry maneuver. The maximum angle of attack is the peak value of the first transient in local angle of attack at the outer wing panel after prospin control inputs. The first peak in angle of attack was used because it is the closest to the initial conditions of the test maneuver and would best enable the influence of such variables as static margin, power, control inputs, and control phasing to be readily detected.

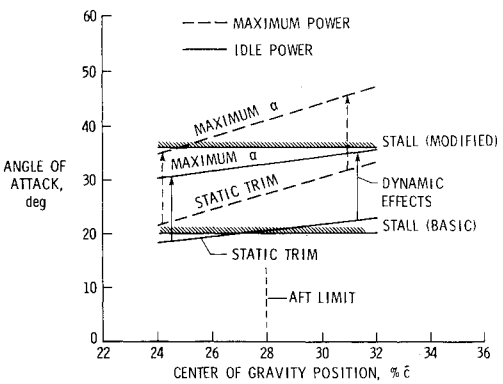

Fig. 10 Attainable outer wing angle of attack for full trailing-edge up stabilator deflection (modified airplane T).

For airplane T (Fig. 10) flight-test results indicated the basic wing outer panel stalled at 20-deg angle of attack. Based on the above assumptions, the intersections of the outer wing angle-of-attack curves and the stall angle-of-attack curves suggest center-of-gravity positions forward of which the airplane should not spin, and aft of which it would have the potential to spin. For example, the airplane with the basic wing would be expected to spin for all center-of-gravity positions shown regardless of power since the maximum angles of attack exceed the stall value of the basic wing. Indeed, the airplane with the basic wing did readily enter spins at 28% mac (the only center-of-gravity position tested for basic airplane T) for both idle and maximum power.

The modified wing outer panel on airplane T stalled at 36-deg angle of attack. According to Fig. 10, airplane T with the modified wing would not be expected to spin at idle and maximum dynamic input until the center-of-gravity position exceeded about 33% mac. For all loadings tested, the modified airplane did not spin with idle power, in general agreement with the data of Fig. 10. Figure 10 also indicates that the airplane would be expected to spin with the use of maximum power and maximum dynamic input with the center of gravity aft of about 25% mac. With maximum power, spin entries were obtained for all loadings tested, including 24% mac; however, it became increasingly difficult to enter a spin as the center of gravity was moved forward and very deliberate, prolonged inputs were required to utilize the dynamic effects to cause spin entry.

The results from airplane R flight tests shown in Fig. 11 indicate similar trends with center-of-gravity and power changes, but with much larger dynamic effects. Flight-test

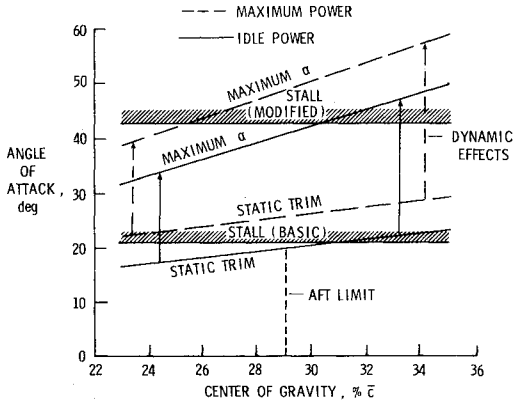

Fig. 11 Attainable outer wing angle of attack for full trailing-edge up stabilator deflection (modified airplane R).

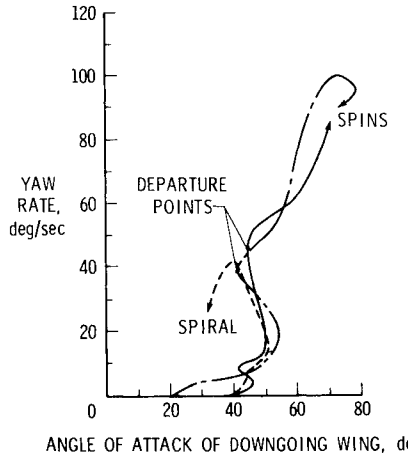

Fig. 12 Yaw rate vs angle of attack for sample spin and spiral maneuvers (modified airplane T).

results showed the basic wing outer panel stalled at about 21-deg angle of attack. Referring to Fig. 11, the basic airplane would be expected to spin for all center-of-gravity positions shown, regardless of power setting. The airplane readily entered spins at 23% mac (the most forward c.g. tested) for both idle and maximum power.

With the wing modification added to airplane R, the outer wing panel stalled at 43-deg angle of attack. According to Fig. 11, this configuration would not be expected to spin for center-of-gravity positions forward of 26% mac even with maximum power and maximum dynamic effects. No spins were obtained during flight tests until the center-of-gravity position was moved aft of 31% mean aerodynamic chord.

The large differences in the dynamic effects exhibited by the two test airplanes indicate that a quantitative measure of spin resistance using only a single parameter such as angle of attack will probably not be adequate. In studies of military aircraft, a technique that has been used to assess spin resistance for a given configuration is to determine combinations of yaw rate and angle of attack which 1) are fully controllable, 2) result in an out-of-control condition (departure), and 3) lead to spin entries. By placing the data points on a yaw rate vs angle-of-attack plot and grouping them, boundaries delineating controlled, departure, and spin entry flight conditions can be determined. Following this approach, flight-test data for airplanes R and T were analyzed in an effort to define a similar boundary. Examples of crossplots of yaw rate and outer wing angle of attack, illustrating both spin and spiral motions for airplane T, are given in Fig. 12.

For each spin there existed a combination of angle of attack and yaw rate beyond which both parameters continued to increase as the airplane proceeded into a fully developed spin. Examples of these departure points are noted on Fig. 12, and departure points for each run examined are summarized in Fig. 13. These data indicate that the wing modification moves the departure points to higher angles of attack, at a given yaw rate, compared to the unmodified airplane. Such a shift is indicative of the improvement in spin resistance afforded by the wing modification.

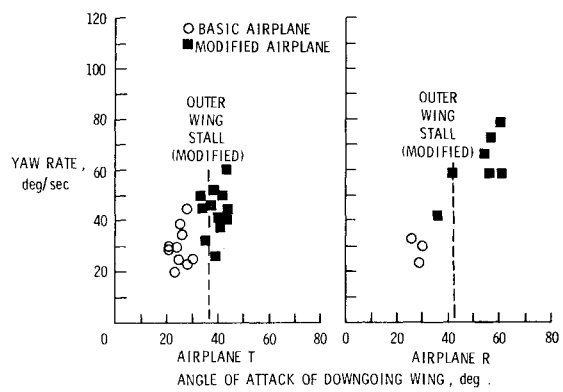

Fig. 13 Values of yaw rate and angle of attack from which spins developed.

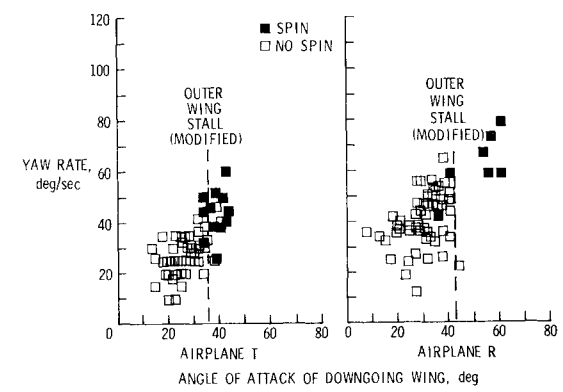

Fig. 14 Peak yaw rates for no-spin cases compared with departure points for the modified airplanes.

Another measure of spin resistance is the time available, following application of prospin controls, for the pilot to take some form of corrective action prior to a spin entry. The elapsed time between prospin control input and reaching the departure point increased from about 4 sec for the basic airplanes to about 10-12 sec for the few cases that did spin with the modified airplanes.

The maximum yaw rate and corresponding angle of attack for maneuvers that did not result in spins, along with the departure points from Fig. 13, are plotted in Fig. 14. This figure shows that in some instances yaw rate and angle of attack reached a level that had the potential for spin entry, but failed to trigger spin entry. Yaw rate and angle of attack are necessary to a spin, but the magnitudes of yaw rate and angle of attack alone are not sufficient to delineate between maneuvers that do and those that do not produce spins. Additional parameters need to be studied to determine how they effect spin resistance so that they can be properly addressed in any design guideline.

The preceding analysis is one step toward providing design guidelines for spin-resistant airplanes. Work in progress is aimed at providing a parameter or combinations of parameters which would predict spin resistance. It is hoped that these parameters would involve ordinary aerodynamic stability and control coefficients which could either be measured during model tests or be estimtated analytically, thus enabling spin-resistance evaluation prior to flight tests.

Summary of Results

Fight tests to evaluate the change in spin resistance due to addition of an outboard wing leading-edge modification to two single-engine airplanes with different basic wing geometries have shown the following results:

1) Use of the modification increased stall angle of attack of the outer wing to approximately double the stall angle of attack of the basic wing.

2) The modified airplanes had improved stall behavior and a high degree of spin resistance compared to the basic airplanes.

3) Spin resistance has been related to both the maximum attainable outer wing panel of attack and the yaw rate generated by the airplane during maneuvers.

4) Spin resistance has been related to center-of-gravity position, power level, and dynamic effects through their influence on the maximum angle of attack attainable at the outer wing panels.

5) For those few maneuvers that did produce spins with the wing modification, the modified airplane took longer than the basic airplane to reach a condition from which it transitioned to the spin, thus providing added time for the pilot to make corrective control inputs.

References

[1]"Exploratory Study of the Effects of Wing Leading-Edge Modifications on the Stall/Spin Behavior of a Light General Aviation Airplane," NASA TP 1589, 1979.

[2]DiCarlo, D. J., Stough III, H. P., and Patton Jr., J. M., "Effects of Discontinuous Drooped Wing Leading-Edge Modification on the Spinning Characteristics of a Low-Wing General-Aviation Airplane," AIAA Paper 80-1843, 1980.

[3]Newsom Jr., W. A., Satran, D. R., and Johnson Jr., J. L., "Effects of Wing Leading-Edge Modifications on a Full-Scale, Low-Wing Airplane—Wind Tunnel Investigation of High Angle-of-Attack Aerodynamic Characteristics," NASA TP 2011, 1982.

[4]Stough, H. P., DiCarlo, D. J., and Stewart, E. C., "Wing Modification for Increased Spin Resistance," SAE Paper 830720, 1983.

[5]White, E. R., "Wind-Tunnel Investigation of Effects of Wing Leading-Edge Modifications on the High Angle-of-Attack Characteristics of a T-Tail Low-Wing General-Aviation Aircraft," NASA CR 3636, 1982.

[6]Knight, M., "Wind-Tunnel Tests on Autorotation and the Flat Spin," NACA 273, 1927.